

# Nonbackscattering Contribution to Weak Localization

A.P. Dmitriev\* and V.Yu.Kachorovskii\*

*Uppsala University, S-751 08, Uppsala, Sweden*

I.V. Gornyi

*A.F.Ioffe Physical-Technical Institute, St.Petersburg, 194021, Russia*

## Abstract

We show that the enhancement of backscattering responsible for the weak localization is accompanied by reduction of the scattering in other directions. A simple quasiclassical interpretation of this phenomenon is presented in terms of a small change in the effective differential cross-section for a single impurity. The reduction of the scattering at the arbitrary angles leads to the decrease of the quantum correction to the conductivity. Within the diffusion approximation this decrease is small, but it should be taken into account in the case of a relatively strong magnetic field when the diffusion approximation is no more valid.

PACS numbers: 73.20.Fz, 72.20.Dp, 72.10.-d

## I. INTRODUCTION

The quantum correction to the conductivity arises from interference of electron waves propagating in opposite directions along closed paths. The interference is destroyed for trajectories which are long enough. In the absence of magnetic field and if spin effects may be neglected it happens due to processes of electron inelastic scattering which are usually taken into account by introducing the phase breaking time  $\tau_\phi$ . At sufficiently low temperatures  $\tau_\phi$  is much greater than the elastic scattering time  $\tau$  and the motion of electrons may be described by a diffusion equation (diffusion approximation).

The corresponding conductivity correction is negative and in the two dimensional case is given by<sup>1</sup>:

$$\Delta\sigma = -\frac{e^2}{2\pi^2\hbar} \ln \frac{L_\phi^2}{l^2}. \quad (1)$$

Here  $L_\phi = (2D\tau_\phi)^{1/2}$  is the phase breaking length,  $D = l^2/(2\tau)$  is the diffusion coefficient and  $l$  is the mean free path.

It is well known<sup>2</sup>, that Eq. (1) allows a simple quasiclassical derivation based on calculation of the probability for an electron to return to the origin.

The presence of magnetic field leads to the phase coherence distortion when the path linear dimensions are larger than the magnetic length  $l_H = (\hbar c/eB)^{1/2}$ . With increasing magnetic field,  $B$ , the magnetic length becomes smaller than  $L_\phi$  and, accordingly, the conductivity correction decreases<sup>3</sup>. For relatively weak magnetic fields, when  $l \ll l_H \ll L_\phi$ , the equation (1) is still valid with  $L_\phi$  being changed by the length of the order of  $l_H$ . For stronger magnetic fields when  $l_H \ll l$  (but still  $l \ll R_c$ ,  $R_c$  is the cyclotron radius), the main contribution to the conductivity correction comes from short closed trajectories with the length of the order of  $l_H$  and the diffusion approximation is no more valid. This case was considered in the Refs. 4,5 and it was found that in two dimensions for short range potential  $\Delta\sigma \propto -l_H/l$ .

The quantitative theory of weak localization is based on the expansion of the conductivity in series of the small parameter  $(k_F l)^{-1}$ , where  $k_F$  is Fermi wave vector. The negative

correction to the conductivity Eq. (1) arises in the first order of this parameter. It can be derived by summing so-called maximally-crossed diagrams (Fig. 1a). These diagrams describe the coherent backscattering of the electron wave. In the case when the diffusion approximation is not valid, together with the diagrams (1a) one should also take into account the diagrams presented in Figs. 1b, 1c and 1d. These diagrams too, give a contribution to the conductivity of the order of  $(k_F l)^{-1}$  but, in contrast to the diagrams (1a), their contribution is positive. The importance of these diagrams were emphasized in many works, but a clear quasiclassical interpretation of processes corresponding to these diagrams was never given. Moreover in Ref. 6 it was claimed that a quasiclassical interpretation of these processes is not possible. In this work we present a simple quasiclassical interpretation of any diagram of the first order in  $(k_F l)^{-1}$ . It is shown that the contribution of these diagrams may be expressed through the classical probability for an electron to return to the origin at a certain angle to the initial direction of motion.

We discuss the possibility of describing weak localization effects in terms of a small change of the differential cross-section of a single impurity. The angular dependence of this modified cross-section for the case of zero magnetic field and the short-range impurity potential is presented in Fig. 2. The positive peak near  $\theta = \pi$  corresponds to the enhancement of backscattering described by the diagrams (1a) while the other diagrams in Fig. 1 are responsible for the decrease of the scattering rate in other directions, the total cross-section remaining unchanged. At the same time the transport cross-section changes and this is the reason for the weak localization corrections. This means that all first order in  $(k_F l)^{-1}$  weak localization effects may be taken into account by changing the differential cross-section of a single impurity. A similar consideration is also possible when magnetic field is applied. In this case the effective cross-section depends on magnetic field.

It is also shown that within the diffusion approximation ( $L_\phi, l_H \gg l$ ) taking into account the diagrams (1b,c and d) leads to the appearance in Eq. (1) of an additional factor  $1/2$  in the argument of the logarithm. At strong magnetic fields ( $l_H < l$ ), when the diffusion approximation is no longer valid, the contribution of the diagrams (1b,c and d) differs from

that of the diagrams (1a) by the numerical factor only.

We calculate numerically the quantum correction to the conductivity for the total range of the classically weak magnetic fields. The results are presented graphically.

The paper is organized as follows. In the first section we give the necessary formulas and definitions. In the second section the derivation of the correction to the conductivity due to the diagrams (1a) is given in the coordinate representation. This method allows to reach more transparent physical presentation. In the third section the quasiclassical interpretation of the rest diagrams in Fig. 1 is given, using the same method. The dependence of the quantum correction on the magnetic field is considered. Finally, in the fourth section we discuss the possibility of describing the weak localization in terms of interference correction to the differential cross-section.

## II. BASIC EQUATIONS

We consider the motion of 2D-electrons in a random potential  $V(\mathbf{r}) = \sum u(\mathbf{r} - \mathbf{R}_i)$ , where  $\mathbf{R}_i$  is a vector of the position of  $i$ 'th impurity,  $u(\mathbf{r})$  is a single impurity potential, which is supposed to be a short-range one. The correlation function of the total potential  $V(\mathbf{r})$  is given by:

$$\langle V(\mathbf{r})V(\mathbf{r}') \rangle = \gamma \delta(\mathbf{r} - \mathbf{r}'). \quad (2)$$

Here the angular brackets denote averaging over the impurity's positions. Static conductivity is calculated with the use of the Kubo formula. It will be convenient for our purposes to write this formula in the coordinate representation:

$$\sigma = -\frac{e^2 \hbar^3}{2\pi m^2 S} \int \int d^2 \mathbf{r}_i d^2 \mathbf{r}_f \left\langle \frac{\partial}{\partial \mathbf{r}_i} G_e^R(\mathbf{r}_i, \mathbf{r}_f, E_F) \frac{\partial}{\partial \mathbf{r}_f} G_e^A(\mathbf{r}_f, \mathbf{r}_i, E_F) \right\rangle. \quad (3)$$

Here  $m$  is the electron mass,  $S$  is the area of the system,  $G_e^{R,A}(\mathbf{r}, \mathbf{r}', E_F)$  are respectively the retarded and advanced exact Green functions at the Fermi energy  $E_F$ .

As is well known, the result of averaging over impurity's positions is represented as a

sum of all the possible diagrams with solid lines corresponding to averaged Green functions and dashed lines corresponding to the potential correlation function.

The expressions for the averaged Green functions are given by

$$G^{R,A}(\mathbf{r}, \mathbf{r}', E_F) = \langle G_e^{R,A}(\mathbf{r}, \mathbf{r}', E_F) \rangle = \int \frac{d^2\mathbf{k} \exp(i\mathbf{k}(\mathbf{r} - \mathbf{r}'))}{(2\pi)^2 (E_F - \frac{\hbar^2 k^2}{2m} \pm \frac{i\hbar}{2\tau})}, \quad (4)$$

where  $\tau = \hbar^3/(m\gamma)$  is the elastic scattering time<sup>7</sup>. These expressions have the following asymptotic behavior at distances exceeding the wave length

$$G^{R,A}(\mathbf{r} - \mathbf{r}', E_F) = \mp \frac{im}{\hbar^2} \frac{1}{\sqrt{2\pi k_F |\mathbf{r} - \mathbf{r}'|}} \exp(\pm i k_F |\mathbf{r} - \mathbf{r}'| - \frac{|\mathbf{r} - \mathbf{r}'|}{2l} \mp i\frac{\pi}{4}). \quad (5)$$

The Green functions  $G^R$  and  $G^A$  describe the divergent and convergent waves respectively. These waves oscillate rapidly on the scale  $k_F^{-1}$  and their amplitudes decrease slowly on the scale of the order of the mean free path  $l$ . The large value of the parameter  $k_F l$  allows to give a quasiclassical interpretation for various terms in the diagram series, the quantity

$$P(\mathbf{r}) = \gamma G^R(\mathbf{r}, E_F) G^A(\mathbf{r}, E_F) = \frac{e^{-r/l}}{2\pi l r} \quad (6)$$

playing an essential role. This is a classical probability density for an electron starting from the origin  $\mathbf{r} = 0$  to experience the first collision around point  $\mathbf{r}$ .

In what follows we will make use of the relation

$$\int d^2\mathbf{r}_i G_{iN}^A \frac{\partial}{\partial \mathbf{r}_i} G_{i1}^R = \frac{i\tau}{\hbar} \frac{\partial}{\partial \mathbf{r}_N} (G_{N1}^R - G_{N1}^A) \approx -\frac{ml}{\hbar^2} \frac{(\mathbf{r}_N - \mathbf{r}_1)}{|\mathbf{r}_N - \mathbf{r}_1|} [G_{N1}^R + G_{N1}^A], \quad (7)$$

which may be easily derived from Eq. (4). Here we use the notation  $G_{jk}^{R,A} = G^{R,A}(\mathbf{r}_j - \mathbf{r}_k)$ .

For a short-range potential, when the scattering is isotropic, the main contribution to the conductivity is given by the diagram without dashed lines, which corresponds to independent averaging of the Green functions in (3). It is easy to see that in this approximation Eq. (3) is reduced to the integral

$$\sigma_0 = \frac{e^2 \tau k_F^2}{2\pi m} \int P(\mathbf{r}_i - \mathbf{r}_f) \frac{d^2\mathbf{r}_i d^2\mathbf{r}_f}{S} = \frac{e^2 n \tau}{m} = \frac{e^2}{2\pi \hbar} k_F l, \quad (8)$$

where  $n$  is the electron concentration. This equation is in fact the classical Drude formula

### III. COHERENT BACKSCATTERING CORRECTION

The coherent backscattering correction to the Drude formula (8) is described, in the first order in  $(k_F l)^{-1}$ , by the diagrams (1a), the number of dashed lines being greater than two<sup>8</sup>.

These diagrams represent the contribution to conductivity related to interference of two processes depicted in Fig. 3a. An electron starting from the point  $i$  reaches the point  $f$  by two ways:

- 1) successively scattering on impurities  $1, 2, \dots, N$ ,
- 2) passing the same chain of impurities in the opposite order  $(N, N-1, \dots, 1)$ .

It means that each section of the trajectory from 1 to  $N$  is passed twice. The amplitudes of these transitions are described by the functions  $G^R$  and  $G^A$  respectively which come into the expression for the conductivity correction as products  $\gamma G^R(\mathbf{r}_j - \mathbf{r}_{j+1}) G^A(\mathbf{r}_j - \mathbf{r}_{j+1}) = P(\mathbf{r}_j - \mathbf{r}_{j+1})$ . Thus the phase difference of the two waves on the paths connecting points 1 and  $N$  is equal to zero and the quantity

$$W_{N-1}(\mathbf{r}_1 - \mathbf{r}_N) = \int d^2\mathbf{r}_2 \dots d^2\mathbf{r}_{N-1} P(\mathbf{r}_1 - \mathbf{r}_2) \dots P(\mathbf{r}_{N-1} - \mathbf{r}_N) \quad (9)$$

appears in the expression for the conductivity correction. This quantity is the classical probability density to find an electron started from point 1 near the point  $N$  after  $N-1$  collisions.

The smallness of the contribution to conductivity of the diagrams (1a) in comparison with the main Drude's one (Eq. (8)) results from the initial and last sections of the trajectories  $(i, 1)$ ,  $(i, N)$  and  $(N, f)$ ,  $(1, f)$  that normally are passed only once (see Fig. 3a). The total phase difference of the two waves at point  $f$  comes from these sections only and is given by

$$\Delta\phi = k_F(|\mathbf{r}_1 - \mathbf{r}_i| + |\mathbf{r}_f - \mathbf{r}_N| - |\mathbf{r}_N - \mathbf{r}_i| - |\mathbf{r}_f - \mathbf{r}_1|). \quad (10)$$

The smallness arises after integrating over the coordinates of the points  $i$  and  $f$  in Eq. (3), due to rapid oscillations of  $\exp(i\Delta\phi)$ . The main contribution to the integral comes from such configurations for which the phase difference is stationary with respect to small variations

of the coordinates of all four key points ( $i$ , 1,  $N$  and  $f$ ). This happens when all these points are close to one line, the points  $i$  and  $f$  lying on the one side from the section 1– $N$  (see Fig. 3b). That is why the processes described by the diagrams (1a) may be interpreted as an additional backscattering on a single impurity (the impurity 1 for the configuration depicted in Fig. 3b).

We stress that it is the condition that the phase difference  $\Delta\phi$  be stationary that is important, but not the condition  $\Delta\phi = 0$ . There are configurations for which  $\Delta\phi = 0$ , but stationarity condition is not valid (for example, when the points  $i$  and  $f$  lie symmetrically with respect to the line 1 –  $N$ ). Such configurations do not contribute to the quantum correction. It turns out however, that in the case presented in Fig. 3b the total phase difference is equal to zero and constructive interference takes place.

The coherent backscattering correction to conductivity can be expressed through the classical probability density for an electron to return to the area of the order  $l\lambda_F$  ( $\lambda_F = 2\pi/k_F$ ) around the impurity 1 (see Appendix A):

$$\Delta\sigma_a = -\sigma_0 \frac{(\lambda_F l)}{\pi} W. \quad (11)$$

Here

$$W = \sum_{N=3}^{\infty} W_N(0) \quad (12)$$

is the sum of probability densities for an electron to return to the origin after 3, 4, .. collisions. In what follows, for the sake of brevity we will name this quantity as the total probability of return<sup>9</sup>.

It is easy to see that

$$W = \int \frac{d^2k}{(2\pi)^2} \frac{P_k^3}{1 - P_k}. \quad (13)$$

Here the quantity  $P_k = (k^2 l^2 + 1)^{-1/2}$  is the Fourier-transform of  $P(\mathbf{r})$ .

The fact that electron should return to the area  $\lambda_F l$  around the impurity 1 can be explained in the following way. The distance between points 1 and  $N$  should be of the order

of  $l$  in consequence of waves fading on the mean free path. Thus only paths which pass at a distance  $(\lambda_F l)^{1/2}$  from impurity 1 (see Fig. 3b) interfere.

Without taking into account the inelastic processes the integral in (12) diverges logarithmically. In order to take into account such processes one can replace  $1/\tau$  by  $(1/\tau + 1/\tau_\phi)$  in the Eq. (4). Then the quantity  $P_k$  is given by

$$P_k = \frac{1}{\sqrt{k^2 l^2 + (1 + \tau/\tau_\phi)^2}}. \quad (14)$$

After integrating in (12) we finally obtain

$$\Delta\sigma_a = -\frac{e^2}{2\pi^2\hbar} \ln \frac{\tau + \tau_\phi}{\tau}. \quad (15)$$

This formula represents the coherent backscattering correction to conductivity.

#### IV. CORRECTION TO THE CONDUCTIVITY DUE TO SCATTERING AT ARBITRARY ANGLE

The set of diagrams which describe the corrections to conductivity of the order of  $(k_F l)^{-1}$  is not restricted by the series of diagrams (1a) only. The diagrams presented in Figs. 1b, 1c and 1d should also be taken into account. In the absence of magnetic field the contributions of such diagrams to the conductivity are of the same absolute value but differ in sign. The contribution of the diagrams of Figs. 1b and 1c is positive whereas the contribution of the diagrams in Fig. 1d is negative. It is easy to show, that magnetic field does not change the contributions of diagrams in Fig. 1c and Fig. 1d and they still compensate each other. Thus, when calculating the correction to conductivity one should take into account only the diagrams in Fig. 1b, both in the presence and in the absence of magnetic field.

Let us show that the process described by diagrams (1b) can be easily interpreted quasiclassically (the diagrams in Figs. 1c and 1d allow a similar interpretation). Such a process is depicted in Fig. 4a. An electron starting from point  $i$  reaches point  $f$  by two ways:

- 1) consecutively scattering by impurities  $1, 2, \dots, N$  and finally by impurity 1 again,



2) scattering in the opposite order by impurities  $N, N-1, \dots, 2$ , and having no collisions at all with impurity 1.

The classical quantities  $P(\mathbf{r}_j - \mathbf{r}_{j+1})$  not containing phase factors correspond to the intervals  $(2, 3), (3, 4), \dots, (N-1, N)$ . The integration over the coordinates of impurities  $3, \dots, N-1$  leads to the appearance of the function  $W_{N-2}(\mathbf{r}_N - \mathbf{r}_2)$ .

The phase difference of the two paths ending at the point  $f$  depends on the lengths of the intervals  $(i, 1), (1, 2), (N, 1), (1, f)$  and  $(i, N), (2, f)$ . and is given by

$$\Delta\phi = k_F(|\mathbf{r}_1 - \mathbf{r}_i| + |\mathbf{r}_2 - \mathbf{r}_1| + |\mathbf{r}_1 - \mathbf{r}_N| + |\mathbf{r}_f - \mathbf{r}_1| - |\mathbf{r}_N - \mathbf{r}_i| - |\mathbf{r}_f - \mathbf{r}_2|). \quad (16)$$

Let us fix the positions of the points  $i, 1, f$  and then integrate over the coordinates of the impurities  $2, N$ . Because of the phase stationarity requirement the contribution to the conductivity arises only from the configurations in which the points  $N$  and  $2$  lie close to the lines  $i-1$  and  $1-f$  respectively in angles of the order of  $(k_F l)^{-1/2}$  (see Fig. 4b). In this configuration  $\Delta\phi$  is equal to zero. It is clear from Fig. 4b that the process described by diagrams (1b) can be interpreted as a coherent changing of the scattering by the impurity 1 at angle  $\theta$ . It can be shown that a reduction of scattering takes place.<sup>10</sup>

The expression for the conductivity correction due to processes of Fig. 4b can be written as (see Appendix B):

$$\Delta\sigma_b = - \sum_{N=3}^{\infty} \frac{\sigma_0}{S\pi} (\lambda_F l) \int d^2\mathbf{r}_1 d^2\mathbf{r}_2 d^2\mathbf{r}_N P(\mathbf{r}_1 - \mathbf{r}_2) W_{N-2}(\mathbf{r}_N - \mathbf{r}_2) P(\mathbf{r}_N - \mathbf{r}_1) \cos\theta, \quad (17)$$

$$\cos\theta = \frac{(\mathbf{r}_N - \mathbf{r}_1)(\mathbf{r}_1 - \mathbf{r}_2)}{|\mathbf{r}_N - \mathbf{r}_1||\mathbf{r}_1 - \mathbf{r}_2|}.$$

Using the Fourier transformation one can get

$$\Delta\sigma_b = \frac{e^2}{\pi\hbar} l^2 \int \frac{d^2k}{(2\pi)^2} \frac{P_k(P'_k)^2}{1 - P_k}, \quad (18)$$

where  $P'_k = (1/kl)(1 - P_k)$  is the Fourier component of the function  $-iP(\mathbf{r}) \cos\alpha$ ,  $\alpha$  is the angle of the vector  $\mathbf{r}$ . Calculating the integral in Eq. (18), we finally obtain:

$$\Delta\sigma_b = \frac{e^2}{2\pi^2\hbar} \left( \frac{\ln 2}{1 + \tau/2\tau_\phi} - \frac{\ln(1 + \tau_\phi/\tau)}{1 + 2\tau_\phi/\tau} \right). \quad (19)$$

Note that this correction is positive in contrast to contribution due to the coherent backscattering. In the diffusion approximation ( $\tau_\phi \gg \tau$ ) the expression (19) simplifies:

$$\Delta\sigma_b = \frac{e^2}{2\pi^2\hbar} \ln 2. \quad (20)$$

The total (with accounting both (1a) and (1b) diagrams) weak localization correction to conductivity in the diffusion approximation is given by

$$\Delta\sigma = -\frac{e^2}{2\pi^2\hbar} \ln\left(\frac{L_\phi^2}{2l^2}\right). \quad (21)$$

Thus when the diffusion approximation is valid the contribution of the diagrams (1b) is logarithmically small compared to the backscattering one and just leads to the appearance of a factor 1/2 in the argument of the large logarithm.

Beyond the diffusion approximation, when only the trajectories with a small number of collisions are important, the situation is quite different. This happens in sufficiently strong magnetic field when the magnetic length  $l_H$  is of the order of the mean free path  $l$ , or less. In this case the correction arising from diagrams (1a) does not contain the large logarithm and contributions of the diagrams (1b) and the diagrams (1a) differ only by a numerical factor of the order of unity.

In the presence of magnetic field, Eqs. (9), (11), (12) and (17) still hold, but the quantity  $P(\mathbf{r} - \mathbf{r}')$  should be replaced by

$$\tilde{P}(\mathbf{r} - \mathbf{r}') = P(\mathbf{r} - \mathbf{r}') \exp(i(e/\hbar c)\mathbf{B}[\mathbf{r} \times \mathbf{r}']).$$

Using Kawabata's method<sup>11</sup> one can expand the functions  $\tilde{P}(\mathbf{r})$ ,  $W(\mathbf{r})$  in terms of the eigenfunctions of a particle of charge  $2e$  in a magnetic field  $B$  and obtain

$$\Delta\sigma = -\frac{e^2}{2\pi^2\hbar} F(x), \quad F(x) = F_a(x) + F_b(x),$$

$$F_a(x) = x \sum_0^\infty \frac{(P_n)^3}{1 - P_n}, \quad F_b(x) = -x \sum_0^\infty \frac{P_n((P_n^1)^2/2 + (P_n^{-1})^2/2)}{1 - P_n},$$

where

$$P_n = \frac{s}{z} \int_0^\infty dt \exp(-st - t^2/2) L_n(t^2),$$

$$P_n^m = \frac{s}{z\sqrt{n + (1 - m)/2}} \int_0^\infty dt \exp(-st - t^2/2) L_n^m(t^2),$$

$x = B/B_0$ ,  $B_0 = \hbar c/(2el^2)$ ,  $s = z(2/x)^{1/2}$ ,  $z = 1 + \tau/\tau_\phi$ ,  $L_n$  and  $L_n^m$  are the Laguerre polynomials. The functions  $F_a(x)$  and  $F_b(x)$  describe the contributions of diagrams (1a) and (1b) respectively. In the high-field limit the quantum correction to conductivity has the form<sup>4,5</sup>

$$\Delta\sigma = \Delta\sigma_a + \Delta\sigma_b = -4.96 \frac{e^2}{2\pi^2\hbar} \frac{1}{\sqrt{x}},$$

$$\Delta\sigma_a = -7.74 \frac{e^2}{2\pi^2\hbar} \frac{1}{\sqrt{x}}, \quad \Delta\sigma_b = 2.78 \frac{e^2}{2\pi^2\hbar} \frac{1}{\sqrt{x}}.$$

Note, that this asymptotical behavior is valid only at very high values of  $x$  and can be hardly observed in experiment.

We have performed numerical calculations of  $\Delta\sigma(B)$  for all range of magnetic fields. The dependencies of  $\Delta\sigma(B)$  and  $\Delta\sigma_a(B)$  for  $\tau_\phi = \infty$  are presented in Fig. 5. The dependence  $\Delta\sigma(B)$  for different values of  $\tau_\phi$  is represented in Fig. 6.

## V. INTERPRETATION OF THE WEAK LOCALIZATION IN TERMS OF CHANGING OF IMPURITY SCATTERING CROSS-SECTION

The method presented above allows to give a transparent interpretation of weak localization effects.

In Refs. 12,13 the effects, described by the diagrams (1a) were treated in the frame of the Boltzman transport equation. The authors of Ref. 13 claim that the main weak localization effect is an effective reduction of elastic scattering time.

Using the ideas of these works it is easy to show that the processes related to diagrams (1b) can be considered in the frame of the Boltzman transport equation as well as coherent backscattering processes. One should just replace the isotropic cross-section  $S_0$  by the following expression:

$$S(\theta) = S_0 + \Delta S(\theta). \tag{22}$$

Here the function  $S(\theta)$  is the modified impurity scattering cross-section which is represented schematically in Fig. 2 and

$$\Delta S(\theta) = \Delta S_a(\theta) + \Delta S_b(\theta).$$

The term

$$\Delta S_a(\theta) = C\Delta(\pi - \theta)$$

corresponds to the coherent backscattering at small angles of the order of  $(k_F l)^{-1}$ . The function  $\Delta(\pi - \theta)$  is concentrated in this angle and the integral of it over  $\theta$  is equal to unity. The quantity  $C$  is expressed through the total probability of return  $W$ :

$$C = \frac{S_0}{k_F l} 4\pi l^2 W. \quad (23)$$

In the diffusion approximation  $W = \ln(\tau_\phi/\tau)/(2\pi l^2)$ .

The function  $\Delta S_b(\theta)$  is negative and corresponds to a decrease of scattering at angle  $\theta$ , being described by the diagrams in Fig. 1b. This function can be expressed through the total probability  $W(\theta)$  for an electron to return to the origin at an angle  $\theta$  to the initial direction of propagation

$$\Delta S_b(\theta) = -\frac{S_0}{k_F l} 4\pi l^2 W(\theta). \quad (24)$$

The return probability  $W(\theta)$  is given by

$$W(\theta) = 2\pi \int r dr r' dr' P(\mathbf{r}) P(\mathbf{r}') \sum_{N=1}^{\infty} W_N(|\mathbf{r} - \mathbf{r}'|). \quad (25)$$

The integration in this equation should be done over absolute values of vectors  $\mathbf{r}, \mathbf{r}'$ , the angle between them being fixed and equal to  $\pi - \theta$ . For  $\tau_\phi \gg \tau$  the straightforward calculation gives

$$W(\theta) = \frac{1}{(2\pi)^2 l^2} \left[ \ln \frac{\tau_\phi}{\tau} - \ln \left| \cos \frac{\theta}{2} \right| - \frac{\pi - |\pi - \theta|}{2} \cot \frac{\theta}{2} \right]. \quad (26)$$

This expression is correct for  $|\pi - \theta| > (k_F l)^{-1}$ . In the opposite case  $\cos(\theta/2)$  in the second term should be replaced by the quantity of the order of  $(k_F l)^{-1}$ . Within the diffusion approximation the main contribution to  $W(\theta)$  comes from the first term in Eq. (26) and

therefore this function is almost isotropic. The anisotropic part of  $W(\theta)$  arises mainly due to triangle trajectories.

It is easy to see from Eqs. (23),(24) and (25) that

$$\int_0^{2\pi} W(\theta)d\theta = W, \quad \int_0^{2\pi} \Delta S(\theta)d\theta = 0. \quad (27)$$

This means, in contrast to the statement in Ref. 13, that the weak localization effects do not change the elastic scattering time, which is inversely proportional to the total cross-section. The reduction of this time due to the coherent backscattering is exactly compensated by its enhancement due to the reduction of the scattering at other angles. This happens due to the fact that each impurity configuration, contributing to coherent backscattering, gives the contribution of the same value to scattering in angle  $\theta$  too (see Figs. 3b and 4b). At the same time, since the differential cross-section is anisotropic due to the quantum corrections (see Fig. 2), the transport scattering time changes and does not anymore equal to the elastic scattering time. This is the physical reason which leads to the quantum corrections to conductivity of the order of  $(k_F l)^{-1}$ .

We want to emphasize that the correct treatment of weak localization effects in the framework of the Boltzman equation is only possible when the diagrams (1b) are taken into account. It can be explained by the following way. For inverse transport scattering time we have

$$\frac{1}{\tau_{tr}} = \frac{1}{\tau S_0} \int_0^{2\pi} S(\theta)(1 - \cos \theta)d\theta = \frac{1}{\tau} + \nu, \quad (28)$$

where the correction  $\nu$  arises due to the term  $\Delta S(\theta)$  in Eq. (22). In the first order in  $(k_F l)^{-1}$  the transport scattering time reads  $\tau_{tr} = \tau(1 - \tau\nu)$ . Then for the conductivity we get the following expression

$$\sigma = \sigma_0 \left[ 1 - \frac{1}{S_0} \int_0^{2\pi} \Delta S(\theta)(1 - \cos \theta)d\theta \right]. \quad (29)$$

It is easy to see that taking into account in this method only the contribution of diagrams (1a) (i.e., assuming that  $\Delta S(\theta) = \Delta S_a(\theta)$ ) leads to the conductivity correction which is twice greater than the correct one.

Using Eq. (27) we obtain for the conductivity correction

$$\Delta\sigma = -\frac{\sigma_0}{2\pi S_0} \int_0^{2\pi} \Delta S(\theta) \cos \theta d\theta = \Delta\sigma_a + \Delta\sigma_b, \quad (30)$$

where

$$\Delta\sigma_{a,b} = \frac{\sigma_0}{2\pi S_0} \int_0^{2\pi} \Delta S_{a,b}(\theta) \cos \theta d\theta. \quad (31)$$

These expressions for  $\Delta\sigma_{a,b}$  coincide with that derived by using the Kubo formula<sup>14</sup>. Note, that after integrating in Eq. (31) the isotropic part of  $\Delta S_b(\theta)$  arising from the first term in Eq. (26) does not contribute to the conductivity. As a result the conductivity correction due to diagrams (1b) does not contain a divergent with  $\tau_\phi$  contribution.

In the presence of magnetic field Eq. (22) remains valid. The quantities  $W$  and  $W(\theta)$  entering Eqs. (23) and (24) should be calculated in this case using Eqs. (9), (12) and (25) in which  $P(\mathbf{r})$  should be replaced by  $\tilde{P}(\mathbf{r})$ . In the high-field limit only triangle paths are important and  $W(\theta)$  is strongly anisotropic and conductivity corrections  $\Delta\sigma_{a,b}$  differ by numerical factor of the order of unity.

## VI. ACKNOWLEDGMENTS

The authors are grateful to M.I.Dyakonov for very useful discussions. This work was supported in part by the Swedish Royal Academy of Science (grant 1240) and by the Russian Foundation for Basic Research (Grant 96-02-17896). Partial support for one of the authors (V.Yu.K.) was provided by a fellowship of INTAS Grant 93-2492-e within the research program of International Center for Fundamental Physics in Moscow. One of the authors (I.V.G.) is grateful to ISSEP for Soros Postgraduate Student Grant. This work was also supported by Grant 1001 within the program "Physics of Solid State Nanostructures". Two of us (A.P.D. and V.Yu.K) express gratitude to Uppsala University for hospitality.

## VII. APPENDIX A

The conductivity correction corresponding to the diagrams (1a) is given by

$$\Delta\sigma_a = - \sum_{N=3}^{\infty} \frac{e^2 \hbar^3}{2\pi m^2 S} \gamma \int d^2 \mathbf{r}_i d^2 \mathbf{r}_f \frac{\partial}{\partial \mathbf{r}_i} G_{i1}^R \frac{\partial}{\partial \mathbf{r}_f} G_{f1}^A \Gamma_{N-1} G_{fN}^R G_{iN}^A d^2 \mathbf{r}_1 \dots d^2 \mathbf{r}_N, \quad (32)$$

where

$$\Gamma_{N-1} = \left( \gamma^{N-1} G_{12}^R G_{12}^A \dots G_{N-1,N}^R G_{N-1,N}^A \right).$$

Using Eqs. (6) and (9) we rewrite the expression (32) as

$$\Delta\sigma_a = - \sum_{N=3}^{\infty} \frac{e^2 \hbar^3}{2\pi m^2 S} \gamma \int d^2 \mathbf{r}_i d^2 \mathbf{r}_f G_{iN}^A \frac{\partial}{\partial \mathbf{r}_i} G_{i1}^R G_{fN}^R \frac{\partial}{\partial \mathbf{r}_f} G_{f1}^A W_{N-1}(\mathbf{r}_1 - \mathbf{r}_N) d^2 \mathbf{r}_1 d^2 \mathbf{r}_N. \quad (33)$$

Using Eq. (7) for integration over  $\mathbf{r}_i, \mathbf{r}_f$  in Eq. (33) we obtain

$$\Delta\sigma_a = - \sum_{N=3}^{\infty} \frac{e^2 n \tau}{m S \pi} (\lambda_F l) \int d^2 \mathbf{r}_1 d^2 \mathbf{r}_2 d^2 \mathbf{r}_N P(\mathbf{r}_1 - \mathbf{r}_2) W_{N-2}(\mathbf{r}_2 - \mathbf{r}_N) P(\mathbf{r}_N - \mathbf{r}_1).$$

Here we neglect the rapidly oscillating products  $G^R G^R$  and  $G^A G^A$ . Finally, using Eqs. (9,12) we derive Eq. (11) presented in the main text.

## VIII. APPENDIX B

The conductivity correction corresponding to the diagrams (1b) is given by

$$\Delta\sigma_b = -2 \sum_{N=3}^{\infty} \frac{e^2 \hbar^3}{2\pi m^2 S} \gamma^2 \int d^2 \mathbf{r}_i d^2 \mathbf{r}_f \frac{\partial}{\partial \mathbf{r}_i} G_{i1}^R \frac{\partial}{\partial \mathbf{r}_f} G_{f2}^A G_{12}^R \Gamma_{N-2} G_{N1}^R G_{iN}^A G_{1f}^R d^2 \mathbf{r}_1 \dots d^2 \mathbf{r}_N, \quad (34)$$

$$\Gamma_{N-2} = \left( \gamma^{N-2} G_{23}^R G_{23}^A \dots G_{N-1,N}^R G_{N-1,N}^A \right).$$

The factor 2 in the Eq. (34) arises due to the consideration of both diagrams (1b) which are complex conjugated to each other. Using (6) and (9) we rewrite the expression (34) as

$$\Delta\sigma_b = -2 \sum_{N=3}^{\infty} \frac{e^2 \hbar^3}{2\pi m^2 S} \gamma^2 \int d^2 \mathbf{r}_i d^2 \mathbf{r}_f G_{iN}^A \frac{\partial}{\partial \mathbf{r}_i} G_{i1}^R G_{12}^R G_{N1}^R G_{1f}^R \frac{\partial}{\partial \mathbf{r}_f} G_{f2}^A W_{N-2}(\mathbf{r}_2 - \mathbf{r}_N) d^2 \mathbf{r}_1 d^2 \mathbf{r}_2 d^2 \mathbf{r}_N. \quad (35)$$

Using Eq. (7) and neglecting the rapidly oscillating functions we get Eq. (17) of the main text.

## REFERENCES

- \* Permanent address: *A.F.Ioffe Physical-Technical Institute, 194021, St.Petersburg, Russia*;  
e-mail: *dmitriev@vip1.ioffe.rssi.ru*
- <sup>1</sup> L.P.Gor'kov, D.E.Khmelnitskii and A.I.Larkin, JETP Letters, **30**, 248 (1979)
- <sup>2</sup> B.L.Altshuler, A.G.Aronov, D.E.Khmelnitskii and A.I.Larkin in: Quantum Theory of Solids, ed. I.M.Lifshits, MIR Publishers, Moscow (1982)
- <sup>3</sup> S.Hikami, A.I.Larkin and Y.Nagaoka, Prog.Theor.Phys. **63**, 707 (1980)
- <sup>4</sup> V.M.Gasparian and A.Yu.Zuzin, Fizika Tverdogo Tela, **27**, 1662 (1985)
- <sup>5</sup> M.I.Dyakonov, Solid State Com. 92, 711 (1994); A.Cassam-Chenai and B.Shapiro, J.Phys. I France **4**, 1527 (1994)
- <sup>6</sup> M.B.Hastings, A.D. Stone, H.U.Baranger Physical Review B, **50**, 8230 (1994)
- <sup>7</sup> There are corrections to the elastic scattering time of the order of  $(k_F l)^{-1}$  and higher due to the renormalization of the imaginary part of the self-energy operator. It is easy to calculate the correction in the first order in  $(k_F l)^{-1}$ . This correction, however, is not related to the weak localization effects, so that we don't consider it in this paper.
- <sup>8</sup> The diagram (1a) with two dashed lines should not be taken into account because in the first order in  $(k_F l)^{-1}$  it is exactly compensated by the sum of two complex conjugated diagrams (1b) with two dashed lines.
- <sup>9</sup> S.Chakravarty and A.Schmid, Physic Reports, **140**, 193 (1986)
- <sup>10</sup> In order to obtain the scattering reduction one should add to  $\Delta\phi$  an additional scattering phase acquired during the first way after two collisions with impurity 1 and take into account the phase factor arising due to integration over the impurity positions near the stationary phase configuration. The resulting phase difference between the two ways is equal to  $\pi$ .



<sup>11</sup> A.Kawabata, J. Phys. Soc. Japan, **53**, 3540 (1984)

<sup>12</sup> T.R.Kirkpatrick, Physical Review B, **33**, 780 (1986)

<sup>13</sup> S.Hershfield and V.Ambegaokar, Physical Review B, **34**, 2147 (1986)

<sup>14</sup> In frame of our interpretation it would be more consistent to define the conductivity corrections due to diagrams (1a) and (1b) as

$$\delta\sigma_{a,b} = -\sigma_0(2\pi S_0)^{-1} \int_0^{2\pi} \Delta S_{a,b}(\theta)(1 - \cos \theta)d\theta,$$

which differ from  $\Delta\sigma_{a,b}$  respectively. However, it follows from Eq. (27) that  $\delta\sigma_a + \delta\sigma_b = \Delta\sigma_a + \Delta\sigma_b$  and such a definition leads to the same result (Eq. (21)) for the total conductivity correction.

## FIGURES

Fig. 1 Diagrams relevant in the first order in  $(k_F l)^{-1}$ : the diagram describing coherent backscattering (a) and the diagrams describing coherent scattering at different angles. The contribution of the diagrams (b) depends on the magnetic field. The contributions of diagrams of the types (c) and (d) compensate each other.

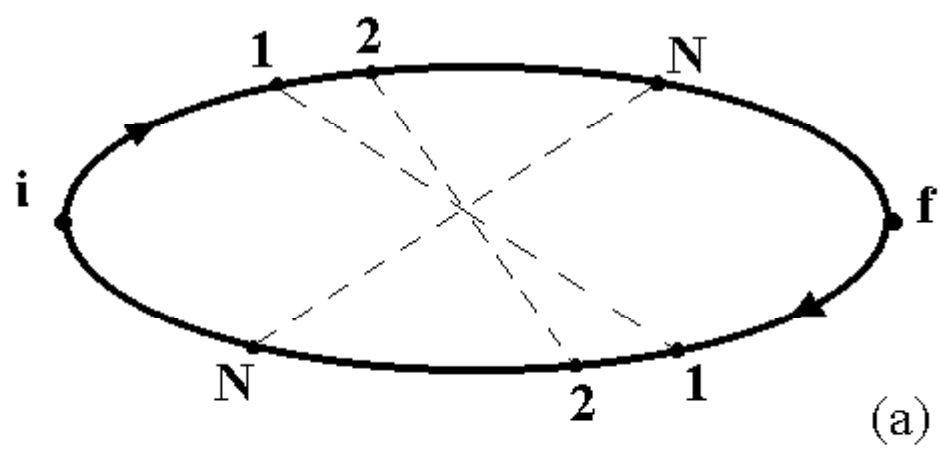
Fig. 2 The angle dependence of the modified differential cross-section on single impurity

Fig. 3 The process related to the diagrams (1a). (a) key points (i, f, 1, and N) have arbitrary positions; (b) the positions of key points satisfy the stationary phase condition

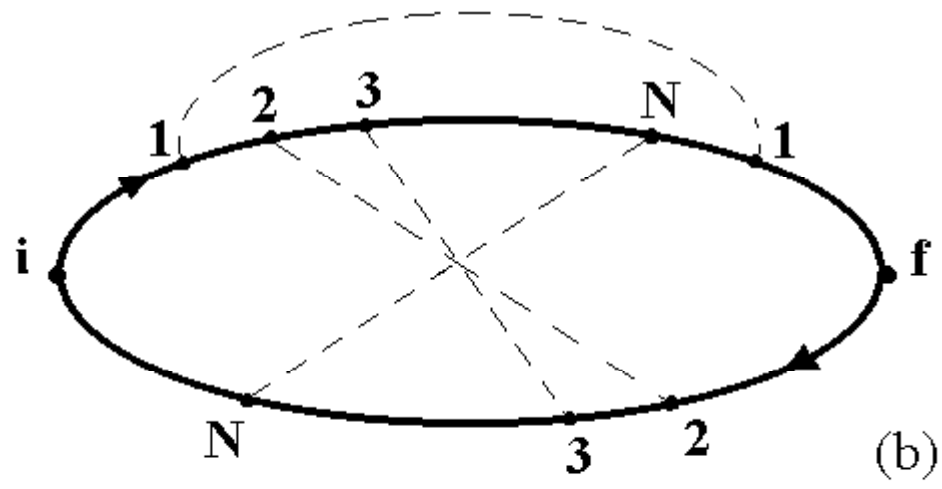
Fig. 4 Similar to Fig. 4, but for the case of the diagrams (1b)

Fig. 5 The conductivity correction dependence on the magnetic field at  $\tau_\phi = \infty$ . The contributions of the diagrams (1a) also is presented.

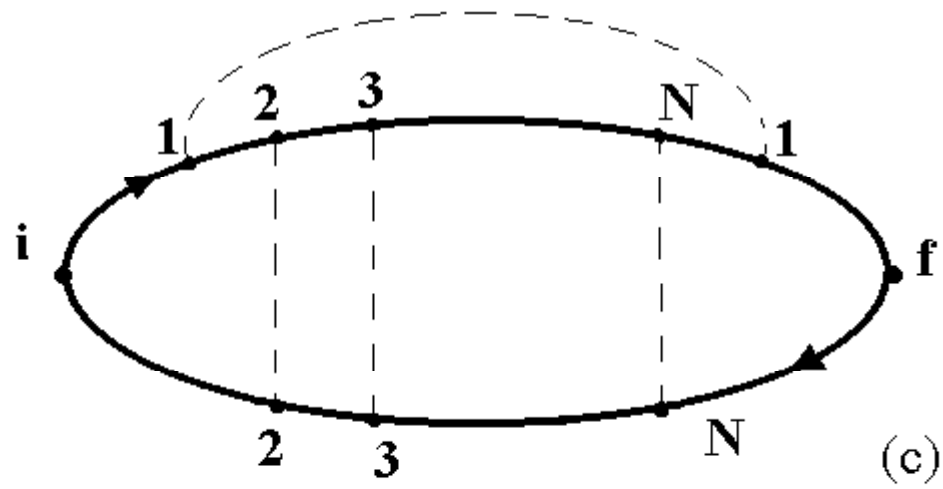
Fig. 6 The conductivity correction dependence on the magnetic field at different breaking phase times





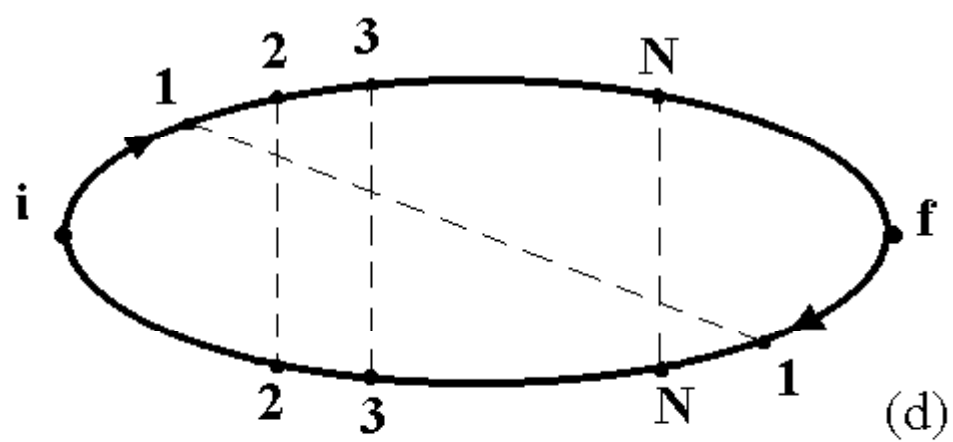




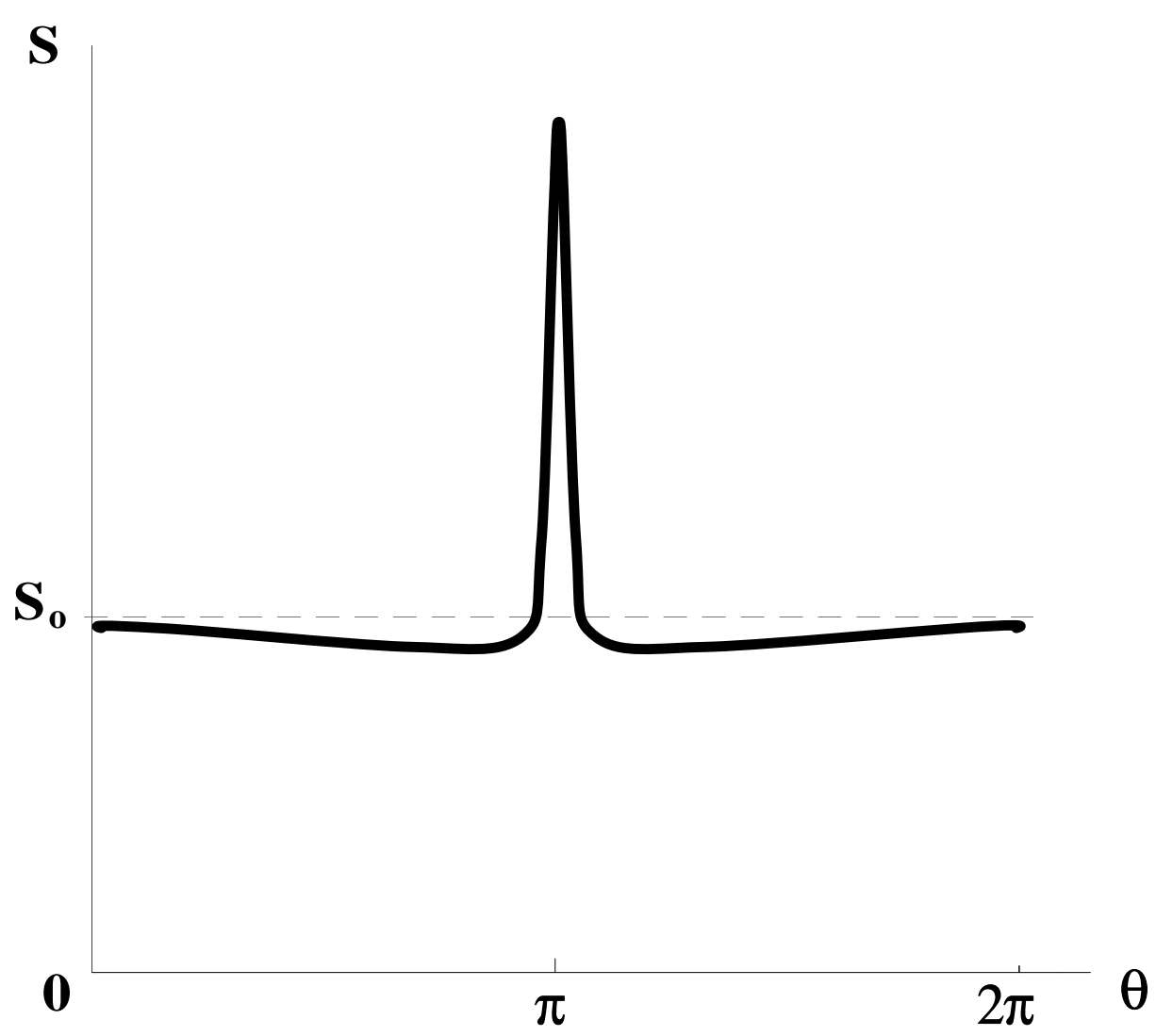


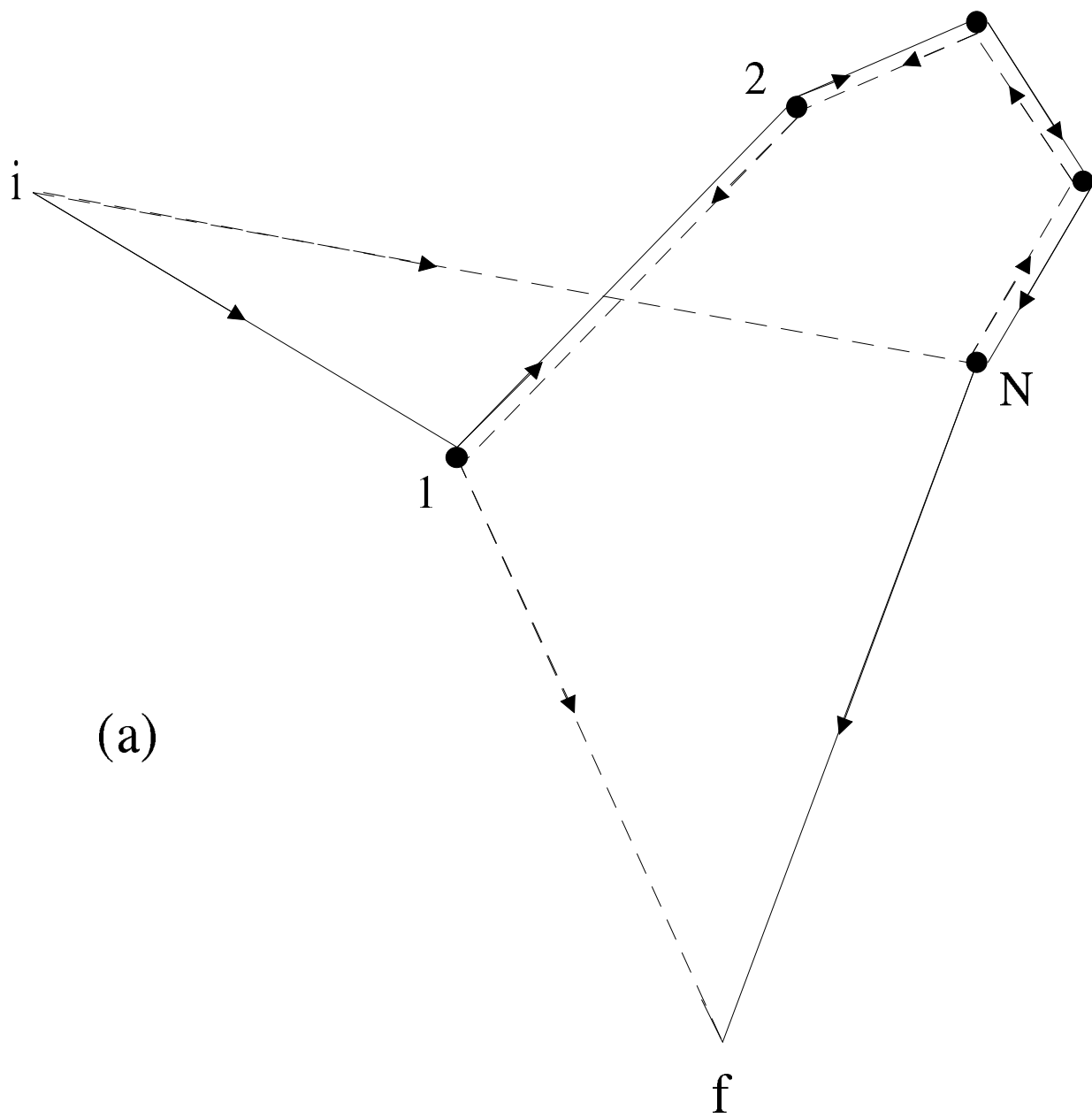




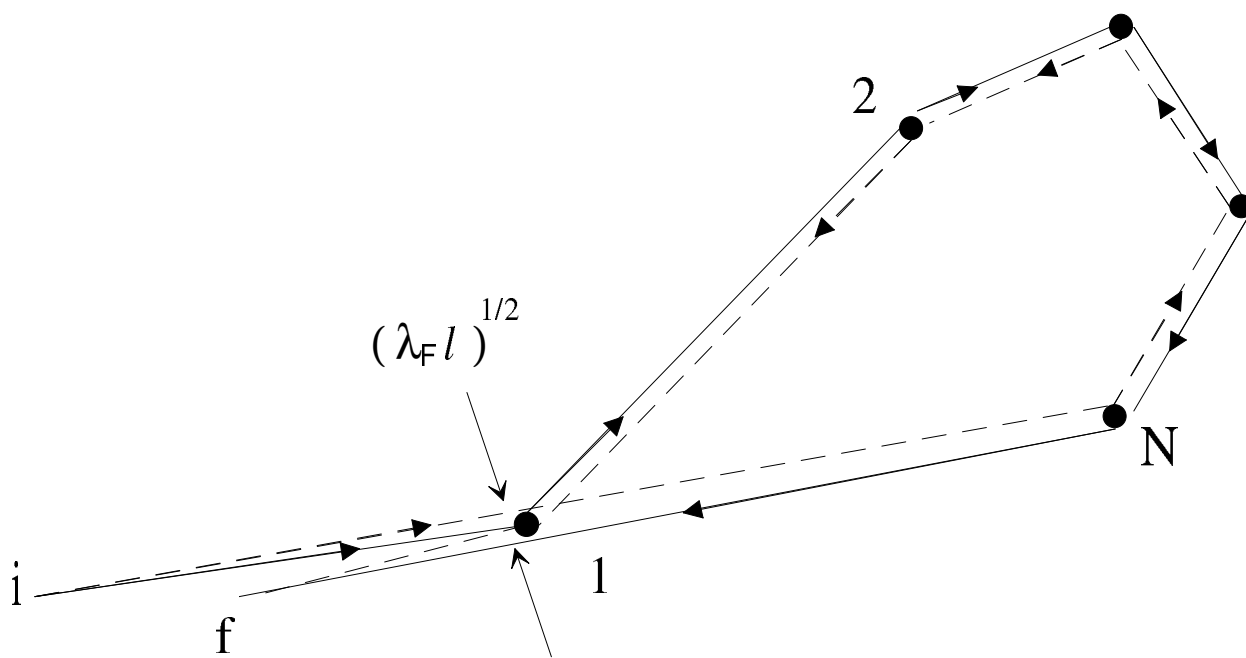




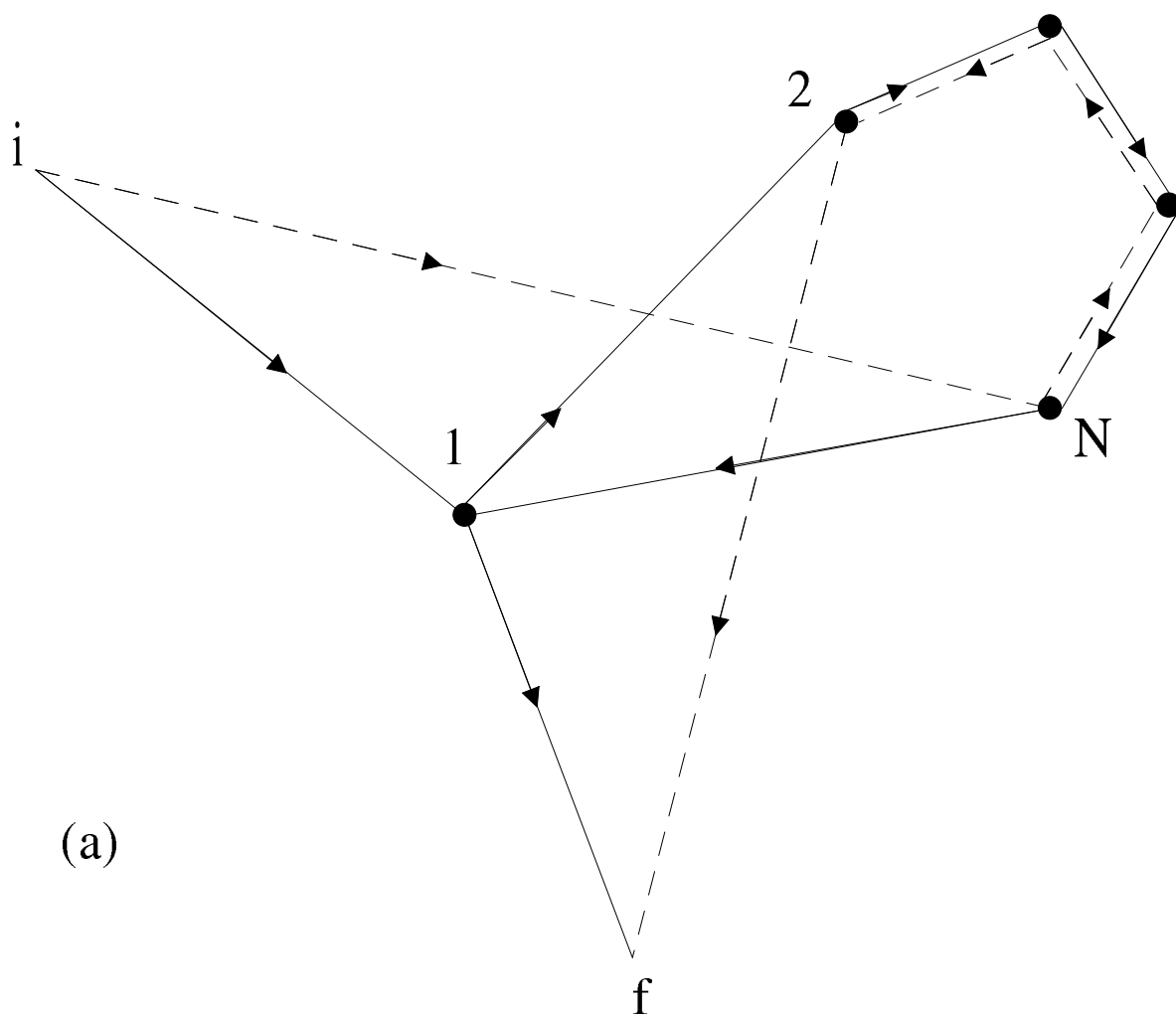




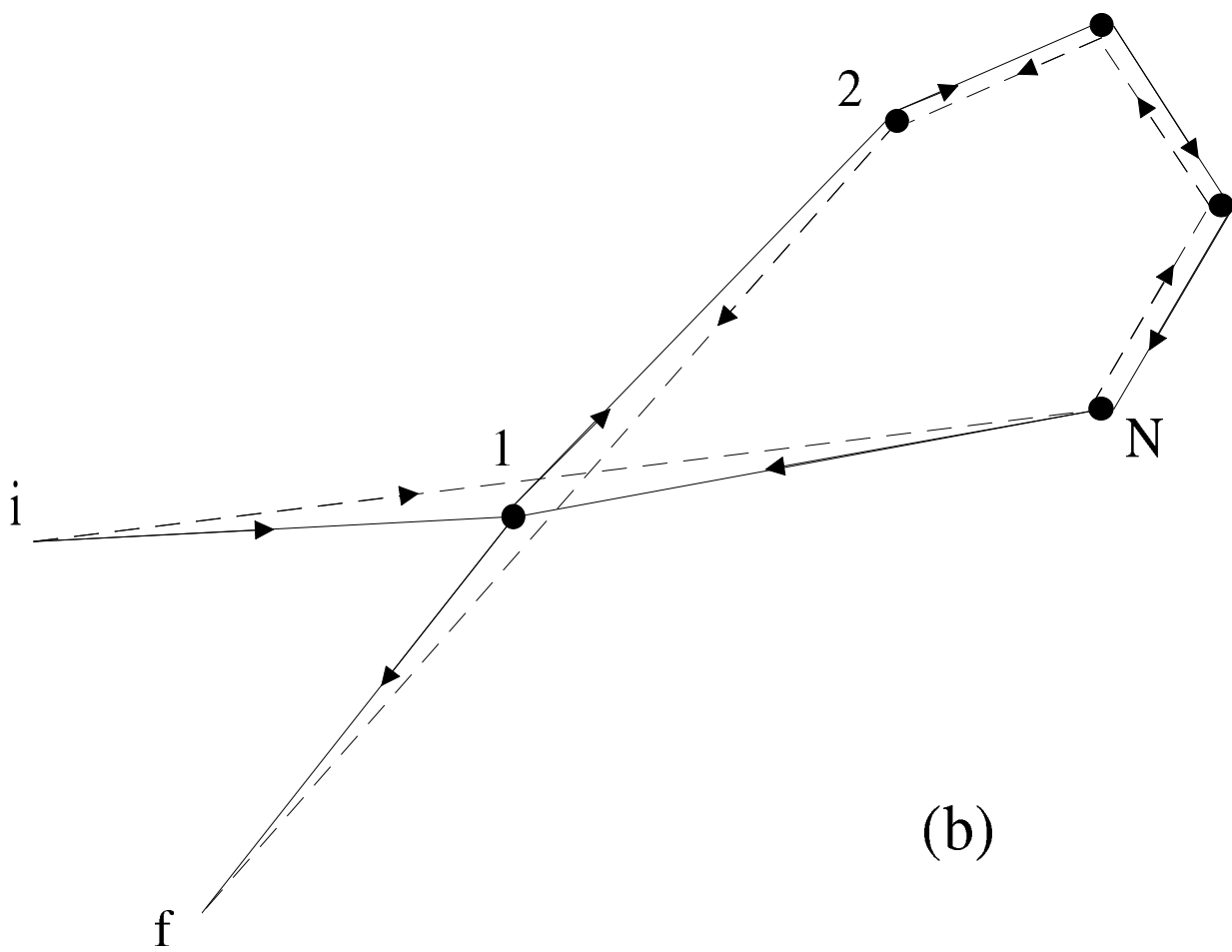
(a)

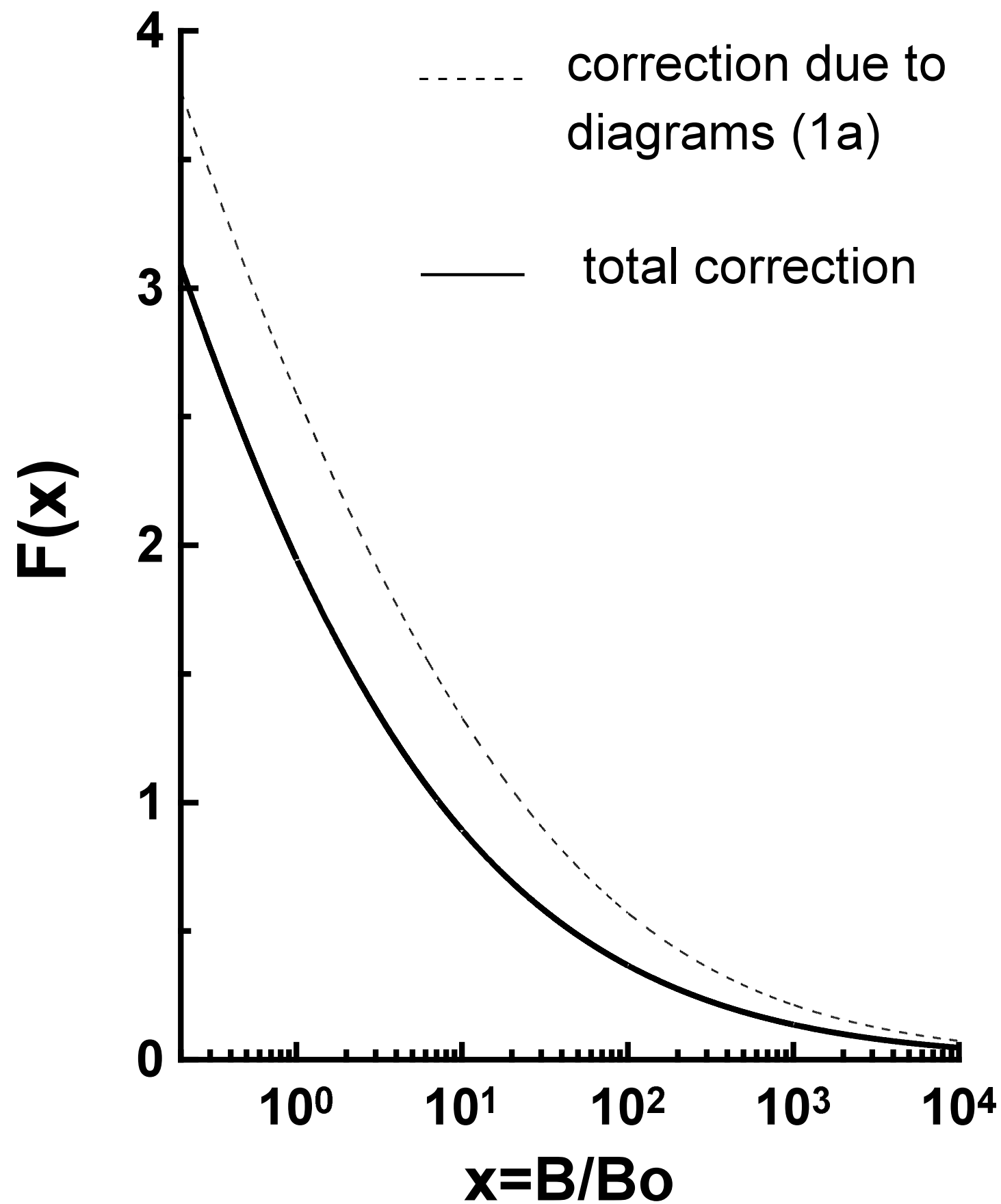


(b)



(a)







$\tau/\tau$  $\phi$ 

0.0

0.01

0.02

0.05

0.1

0.2

0.3

